AGU PUBLICATIONS

Geophysical Research Letters

RESEARCH LETTER
10.1002/2014GL060979

Key Points:
- The water column is important in our understanding of microseism propagation
- Pinch out at the shelf edge reflects back most microseism energy
- Microseisms observed on land are dominated by near-coastal wave activity

Supporting Information:
- Readme
- Text S1
- Animation S1
- Figure S1
- Figure S2

Correspondence to:
C. J. Bean,
chris.bean@ucd.ie

Citation:
Ying, Y., C. J. Bean, and P. D. Bromirski (2014), Propagation of microseisms from the deep ocean to land, *Geophys. Res. Lett.*, *41*,6374–6379, doi:10.1002/2014GL060979.

Received 24 JUN 2014
Accepted 30 AUG 2014
Accepted article online 3 SEP 2014
Published online 22 SEP 2014

Propagation of microseisms from the deep ocean to land

Yingzi Ying[1], Christopher J. Bean[1], and Peter D. Bromirski[2]

[1]Seismology Laboratory, School of Geological Sciences, University College Dublin, Dublin, Ireland, [2]Scripps Institution of Oceanography, University of California, San Diego, La Jolla, California, USA

Abstract Ocean-generated microseisms are faint Earth vibrations that result from pressure fluctuations at the sea floor generated by the interaction between ocean surface gravity waves, and are continuously recorded as low frequency seismic noise. Here we investigate microseism propagation away from deep-ocean source regions using the spectral element method for an oceanic model that contains realistic northeast Atlantic Ocean irregular-layered structure composed of water, sediment, and upper crust. It also includes structural heterogeneities and continental slope and shelf bathymetry. Numerical simulations of coupled acoustic and elastic wave propagation in both simplified models and the full realistic model show that most microseism energy is confined to sediment and water column waveguides. We also show that a significant portion of microseism energy is reflected back to the deep ocean by the continental slope, while only a small fraction of deep-ocean-generated microseism energy reaches land. We conclude that terrestrially observed microseisms are largely generated in shallow water on continental shelves.

1. Introduction

Pressure fluctuations at the ocean floor caused by ocean water waves generates ubiquitous microseisms [*Aster et al.*, 2010; *Bromirski*, 2009; *Traer et al.*, 2012]. Microseism spectra normally show two predominant peaks corresponding to different mechanisms: (i) primary microseisms, with the same period as water waves, are generated by ocean gravity waves incident on a sloped bottom in shallow water [*Hasselmann*, 1963]; and (ii) secondary microseisms, which have much greater amplitude at half the period of the gravity waves, arise from the nonlinear interaction of gravity wave trains traveling in nearly opposite directions [*Longuet-Higgins*, 1950; *Ardhuin et al.*, 2011].

Microseisms are considered to propagate predominantly as Rayleigh waves [*Longuet-Higgins*, 1950; *Hasselmann*, 1963], but some Love waves can also be excited due to structural heterogeneity [*Saito*, 2010]. Using seismic array analyses, *Gerstoft et al.* [2008] also observed that microseisms originating in the deep ocean generate body waves that propagate through the Earth's mantle and core. *Bromirski et al.* [2013] observed that secondary microseisms rarely propagate from deep ocean to land by comparisons between spectra from microseisms recorded on ocean bottom and continental stations. To further explore differences in secondary microseism propagation, first, we use numerical simulations to investigate the influence of layered oceanic geological structures, such as a thin or thick water column and sediments, on microseism propagation across oceanic regions. Next we investigate the process of microseism propagation from deep ocean to land using a realistic geological model from the northeast Atlantic, particularly focusing on evaluating the effects of traversing from deep water across the continental shelf.

We employ the spectral element method, which has very good accuracy and convergence properties and has become an increasing popular approach in computational seismology in the past decade [*Komatitsch and Vilotte*, 1998; *Tromp et al.*, 2008]. The spectral element method is capable of modeling wave propagation in coupled fluid-solid structures using domain decomposition [*Komatitsch et al.*, 2000], which enables simulating the forward propagation of microseisms for a realistic ocean geological model. Although microseisms are generated beneath an entire storm region, here we consider only a single point source in both space and time in order to simplify the problem and allow investigation of microseism propagation characteristics.

2. Effects of Layered Structures on Microseism Propagation

Secondary microseisms can originate farther offshore and in much deeper water than primaries [*Bromirski et al.*, 2005]. The water layer only supports acoustic waves and is typically underlain by a sedimentary layer

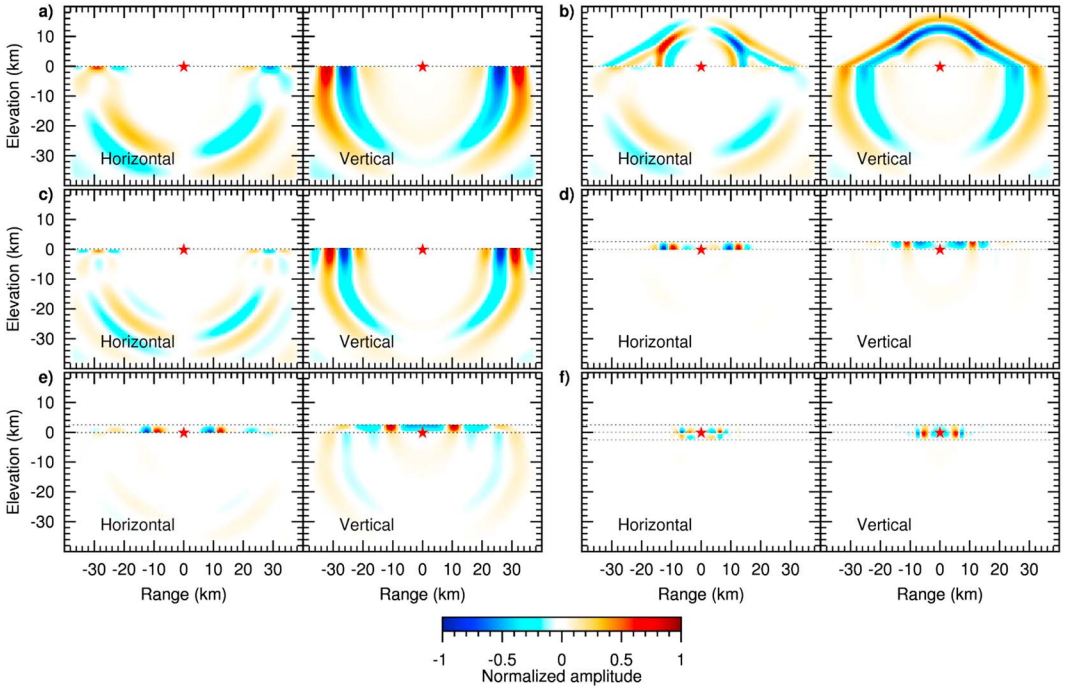

Figure 1. Snapshots of horizontal and vertical displacement wavefields at 15 s using the simplified seismic models: (a) crustal half-space; (b) water half-space over crustal half-space; (c) thin water layer over a crustal half-space; (d) thick water layer over crustal half-space; (e) sandwich structure with thick water layer, thin sediment layer, over a crustal half-space; and (f) sandwich structure with thick water and thick sediment layers over a crustal half-space. The thicknesses for the thin and thick sediment/water layers are set to be 250 m and 2.5 km, respectively. The source (red star) is located at the origin of the coordinate system for all cases. Snapshots are normalized by the maximum absolute value between the horizontal and vertical components.

that supports both compressional and shear wave propagation. The oceanic structure consists of water, sediment, and crustal layers that form a waveguide, and we will evaluate its effects on microseism propagation through numerical simulations initially with simplified models.

We start with the simplest case, i.e., a crustal half-space with a stress-free surface at which both the normal and shear tractions vanish. The crust consists of a homogeneous solid having material density, *P* wave velocity, and *S* wave velocity of 3 g cm^{-3}, 6 km s^{-1}, and 3.5 km s^{-1}, respectively. Sediment density, *P* wave, and *S* wave velocities of sediment are 2.0 g cm^{-3}, 2.5 km s^{-1}, and 1.0 km s^{-1}, respectively, and the density and sound speed of seawater are given by the values of 1.02 g cm^{-3} and 1.5 km s^{-1}, respectively. The Stacey conditions [*Stacey*, 1988] are applied to suppress numerical reflections from the absorbing boundaries of the computational domain. A vertical single force with a Ricker wavelet of 5 s half duration is applied inside the elastic layer to simulate a microseism source in all cases. Here a short-duration wavelet is adopted instead of a continuous signal to facilitate easy analysis of propagation effects. Figure 1a depicts a snapshot of the displacement wavefields showing Rayleigh waves are excited at the free surface, which diverge from *S* waves in the far field due to their velocity difference.

Microseisms result from the interaction of ocean gravity-wave-induced pressure signals with the solid Earth. One important feature of the oceanic environment for microseism propagation is the fluid-solid coupling; the boundary conditions should satisfy the continuity of normal displacement and normal traction, and tangential traction vanishes. In addition to generating Scholte waves that propagate along the fluid-solid interface, seismic phases on the ocean floor will couple elastic energy into acoustic waves that radiate into the water column that are termed leaky Rayleigh waves [*Zhu et al.*, 2004] or acoustic pseudo-Rayleigh waves [*Bromirski et al.*, 2013]. The wavefield snapshot for a coupled model consisting of a water half-space over a crustal half-space is shown in Figure 1b. For consistency, we express the wavefields both in the fluid and solid domains using particle displacement. Acoustic waves are generated in the fluid half-space, and consequent energy loss from interaction with the seafloor contributes to displacement amplitude decay

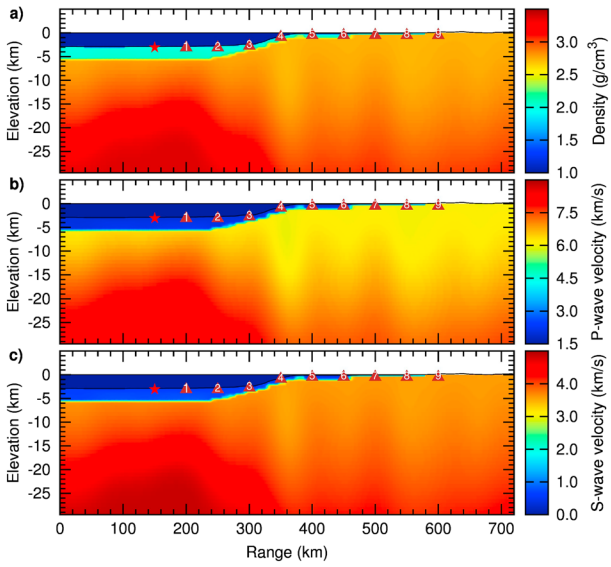

Figure 2. Two-dimensional seismic model of the northeast Atlantic Ocean west of Ireland: (a) density structure, (b) *P* wave velocity structure, and (c) *S* wave velocity structure. The source (red star) is located 1 m below the ocean floor at range 150 km, and a linear seismographic station array (brown triangles) is deployed following the bathymetric profile with 50 km horizontal spacing. The transect is oriented east-west at latitude 54.85°N between longitudes 13.60°W and 7.12°W. The coast is at 580 km range.

with propagation distance. We can also see that the horizontal displacements are discontinuous on the fluid-solid interface.

Of course, oceans on the Earth are not infinitely deep but are "thin" in shallow water and relatively "thick" in the deep ocean compared to an acoustic wavelength in the microseism band. The ocean surface is a pressure-release boundary, which has zero sound pressure because the reflected wave has a π phase reversal with respect to the incident wave. Our shallow water geological model consists of a 250 m thick water layer above a crustal half-space. Figure 1c shows a snapshot of horizontal and vertical displacements of the microseism wavefield. Most microseism energy propagates in the elastic crust, and the thin water layer plays a trivial role in microseism propagation.

In contrast, in our simplified deep-ocean geological model, a 2.5 km thick water layer overlies a crustal half-space. The snapshot in Figure 1d shows that seismic waves in the water column are multiply reflected between the free surface and ocean bottom. The deep-ocean water layer forms a waveguide that confines the propagation of most microseism wave energy.

Another important structural feature of the deep-ocean geological model is the sedimentary layer, which can range from hundreds to thousands of meters in thickness [*Divins*, 2003]. First, we investigate the response of our simplified model by inserting a 250 m thick sedimentary layer at the base of a thick water layer, overlying a crustal half-space (Figure 1e). The solid-solid interface between sediment and crust can preserve the continuity of displacements and the tractions both in the normal and the transverse directions. For the model parameters used, the thin sedimentary layer seems not to be important for microseism propagation, as its vertical dimension is much less than a Rayleigh wave wavelength.

Next we increase the sediment thickness to 2.5 km to reflect a more realistic layered structure representative of a deep-ocean geological model in the northeast Atlantic Ocean off the Irish shelf. Most microseism energy is trapped in the waveguide formed by the combined thick water layer and thick sedimentary layer, shown in Figure 1f. The dominant portion of microseism energy is attributed to leaky Rayleigh wave modes, which normally propagate at slightly lower phase velocities than the *S* wave velocity of the sediment. Furthermore, the multiple reflections cause the propagation path to be much longer than the horizontal propagation range, such that the main "group energy" of microseisms propagates slowly in thickly sedimented ocean regions.

3. Propagation in a Realistic Northeast Atlantic Ocean Geological Model

Thus far, we have not incorporated structural heterogeneities within the sediment and crustal layers, nor bathymetry, whose main feature is the transition zone between the deep ocean and shallow water, i.e., a continental slope. These features are incorporated in a 2-D model of the northeast Atlantic Ocean west of Ireland (Figure 2), at latitude 54.85°N between longitudes 13.60°W and 7.12°W. The regional density structure (Figure 2a) was obtained from the free-air gravity inversion [*Kim et al.*, 2010]. The *P* wave and the *S* wave velocity structures, shown in Figures 2b and 2c, respectively, were determined from the density model using empirical relationships [*Brocher*, 2005]. A realistic bathymetry with 30 arc sec resolution ("The GEBCO_08 Grid," http://www.gebco.net/) was also incorporated to better represent the fluid-solid interface in our model. A vertical point source represented by a 5 s half-duration Ricker wavelet acting 1 m below the

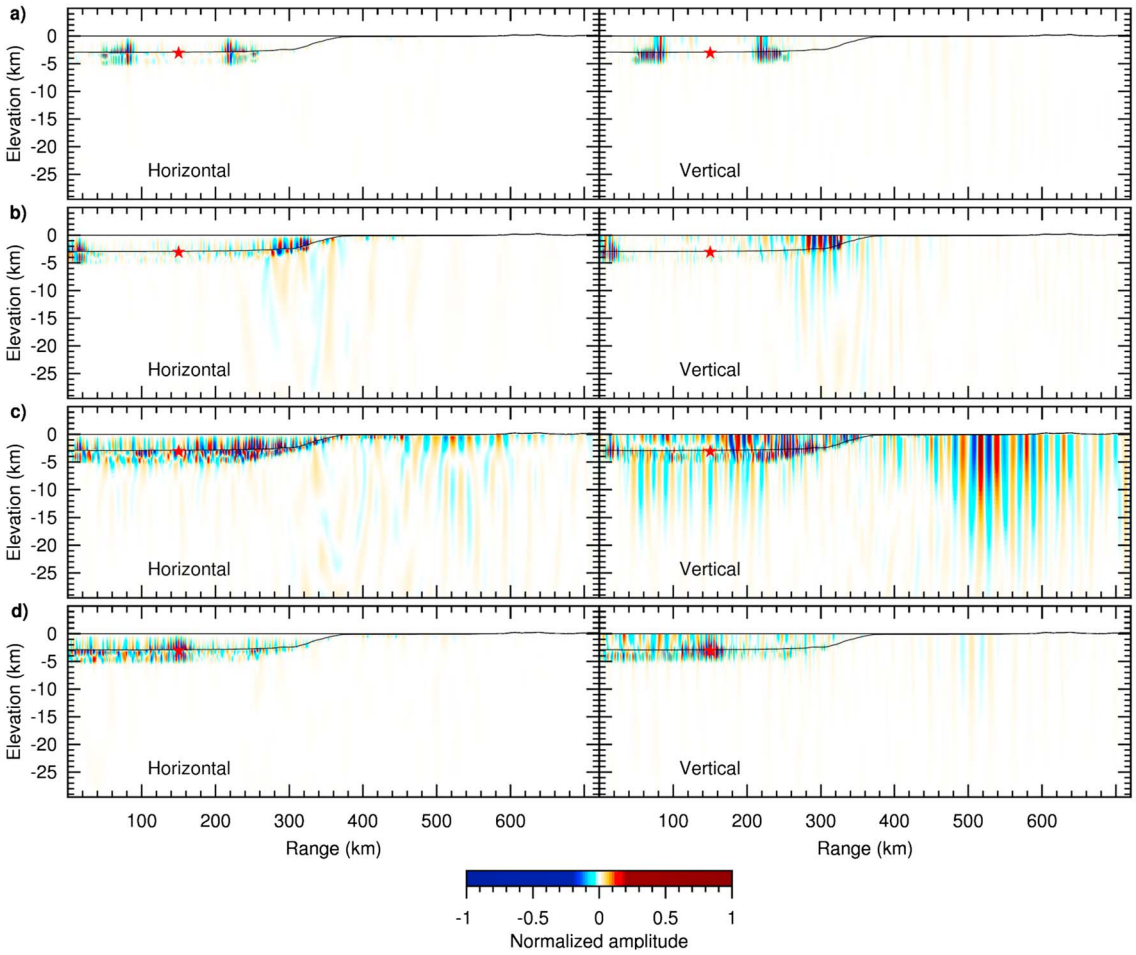

Figure 3. Horizontal and vertical displacement snapshots at (a) $t = 180$ s, (b) $t = 360$ s, (c) $t = 450$ s, and (d) $t = 720$ s of the microseism wavefields propagating in the northeast Atlantic Ocean geological model (Figure 2). A wavefield propagation animation is presented in the supporting information. The coast is at 580 km range.

seafloor simulates the microseism noise source, whose frequency band is roughly in [0.095, 0.35] Hz. The microseism response is measured by a nine-station linear array following the bathymetric profile placed 1 m below the seafloor at 50 km horizontal spacing.

Several snapshots of displacement wavefields excited by the source illustrate microseism propagation in this realistic model. The color axis is scaled to make the weak background seismic wave amplitude variation more visible. Figure 3a is a snapshot at $t = 180$ s, showing that the wave amplitudes remain elevated in the deep-ocean waveguide composed of water and sedimentary layers, and the wave structure exhibits reverberations due to multiple reflections. Some microseism energy can propagate along the sediment-crustal basement interface in the deep ocean as Stoneley waves. A portion of secondary microseisms propagating in the deep-ocean waveguide penetrates the continental slope, as shown in Figure 3b at $t = 360$ s.

At $t = 450$ (Figure 3c), the deep-ocean-generated microseisms transition the shallow water shelf region and continue to propagate onto land as Rayleigh waves. To the east of the continental shelf break at ranges between about 400 and 550 km, the thin shallow water layer, whose depth is far less than a microseism wavelength, plays a trivial role in microseism propagation and can be ignored. A significant portion of the microseism energy is reflected by the continental slope back into deep-ocean waveguide consistent with *Stephen et al.* [2013], as shown by the snapshot at $t = 720$ s (Figure 3d). The full propagation process is illustrated in an animation in the supporting information.

The horizontal and vertical displacement seismograms measured along the seismographic station array are shown in Figure 4. These traces clearly show the propagation and continental slope reflection patterns.

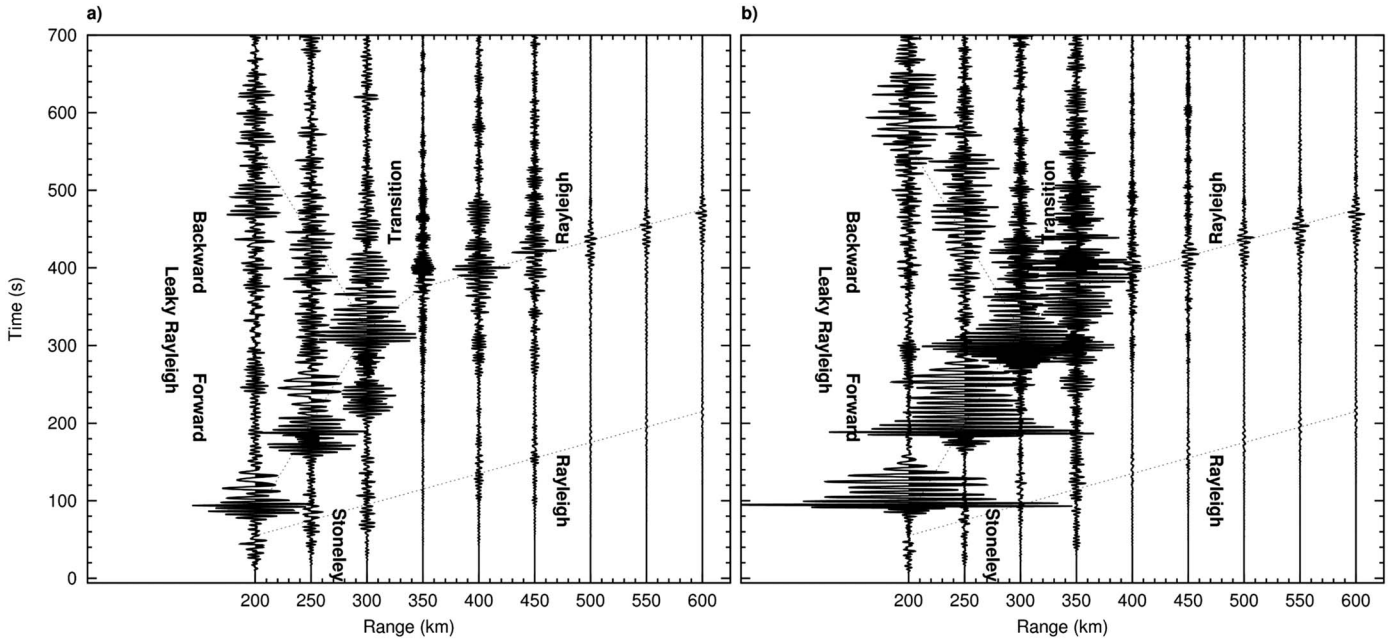

Figure 4. (a) Horizontal and (b) vertical displacement signals recorded by the seismographic station array shown in Figure 2. The group velocity of Stoneley waves in deep-ocean region and Rayleigh waves in shallow water and on land are about 2.6 km/s, which approximates the *S* wave velocity of the upper crust. The group velocity of leaky Rayleigh waves in waveguides is about 0.4 km/s. Strong reflections from the pinch out at the shelf break can be seen, especially on the vertical components.

The waveform envelopes are gradually prolonged when propagating in the deep-ocean waveguide because of multiple reflections. A significant portion of microseism energy is reflected back by the continental slope, demonstrating that only a small portion of microseism energy originating in the deep ocean will reach land stations. Only about 0.2% of the displacement energy recorded on the deep-ocean floor at range 200 km is observed on land at range 600 km (20 km onshore). From the time delays between the envelopes recorded by the equally spaced stations, we see that microseisms propagate slowly in the deep-ocean waveguide but speed up in shallow water region and on land. Only a relatively small amount of Stoneley wave energy, which propagates along sediment-crust interface, arrives first at the land stations.

4. Discussion and Conclusions

Several recent studies have addressed microseism propagation from the deep ocean to land [e.g., *Obrebski et al.*, 2012; *Bromirski et al.*, 2013]. Spectral element method seismoacoustic modeling presented here of the Atlantic coastal region west of Ireland indicates that microseism energy observed on land is dominated by near-coastal wave activity, in agreement with *Bromirski and Duennebier* [2002]. Furthermore, these results confirm that coastal wave activity levels can likely be well estimated from microseism variability measured by near-coastal seismic stations [*Bromirski et al.*, 1999].

Seismic wave attenuation was not included in the simulations presented above. The results for viscoelastic simulations are presented in the supporting information (Figures S1 and S2). The reflections propagating back into deep ocean from the pinch out at the continental shelf break are somewhat damped. However, the same basic features seen in the elastic simulations are still present. Microseism propagation from the deep ocean to land, across a shelf break, is a highly inefficient process.

The numerical results of secondary microseisms in simplified crustal models and for a realistic northeast Atlantic Ocean geological model were investigated to determine their propagation characteristics when transitioning across a continental slope from deep water to land. Microseisms propagate in the form of coupled acoustic and elastic waves in the deep-ocean environment. Most microseism energy is confined in the deep-ocean waveguide and propagates at low group velocities, in part, because multiple reflections occur within the waveguide. Some microseisms originating in the deep ocean can propagate along the sediment-crust interface as Stoneley waves, transitioning the continental slope and arriving on land first.

The spectral element simulation results show that thin shallow water and sediment layers are generally not important, and their effects need not be considered. Continental slopes reflect a significant portion of microseism energy back into the deep ocean, and only a very small portion transitions into shallow water and continues to propagate on land at higher Rayleigh wave propagation speeds.

Acknowledgments

This work was supported by the QUEST Initial Training Network funded within the European Union Marie Curie Programme, a Science Foundation Ireland Principal Investigator Award through the Wave-Obs project, and Peter D. Bromirski received NSF support through grant OCE-1030022. The authors wish to acknowledge Irish Centre for High-End Computing for the provision of computational facilities and support. Thanks to Brian O'Reilly for providing the density model and helpful discussions.

The Editor thanks two anonymous reviewers for their assistance in evaluating this paper.

References

Ardhuin, F., E. Stutzmann, M. Schimmel, and A. Mangeney (2011), Ocean wave sources of seismic noise, *J. Geophys. Res.*, *116*, C09004, doi:10.1029/2011JC006952.

Aster, R. C., D. E. McNamara, and P. D. Bromirski (2010), Global trends in extremal microseism intensity, *Geophys. Res. Lett.*, *37*, L14303, doi:10.1029/2010GL043472.

Brocher, T. M. (2005), Empirical relations between elastic wavespeeds and density in the Earth's crust, *Bull. Seismol. Soc. Am.*, *95*(6), 2081–2092.

Bromirski, P. D. (2009), Earth vibrations, *Science*, *324*(5930), 1026–1027.

Bromirski, P. D., and F. K. Duennebier (2002), The near-coastal microseism spectrum: Spatial and temporal wave climate relationships, *J. Geophys. Res.*, *107*(B8), 2166, doi:10.1029/2001JB000265.

Bromirski, P. D., R. E. Flick, and N. Graham (1999), Ocean wave height determined from inland seismometer data: Implications for investigating wave climate changes in the NE Pacific, *J. Geophys. Res.*, *104*(C9), 20,753–20,766.

Bromirski, P. D., F. K. Duennebier, and R. A. Stephen (2005), Mid-ocean microseisms, *Geochem. Geophys. Geosyst.*, *6*(4), Q04009, doi:10.1029/2004GC000768.

Bromirski, P. D., R. A. Stephen, and P. Gerstoft (2013), Are deep-ocean-generated surface-wave microseisms observed on land?, *J. Geophys. Res. Solid Earth*, *118*, 3610–3629, doi:10.1002/jgrb.50268.

Divins, D. (2003), NGDC total sediment thickness of the world's oceans and marginal seas, NOAA Natl. Geophys. Data Cent., Boulder, Colo.

Gerstoft, P., P. M. Shearer, N. Harmon, and J. Zhang (2008), Global P, PP, and PKP wave microseisms observed from distant storms, *Geophys. Res. Lett.*, *35*, L23306, doi:10.1029/2008GL036111.

Hasselmann, K. (1963), A statistical analysis of the generation of microseisms, *Rev. Geophys.*, *1*(2), 177–210.

Kim, W. J., P. M. Shannon, B. M. O'Reilly, and J. Hall (2010), Lithospheric density variations and Moho structure of the Irish Atlantic continental margin from constrained 3-D gravity inversion, *Geophys. J. Int.*, *183*(1), 79–95.

Komatitsch, D., and J.-P. Vilotte (1998), The spectral element method: An efficient tool to simulate the seismic response of 2D and 3D geological structures, *Bull. Seismol. Soc. Am.*, *88*(2), 368–392.

Komatitsch, D., C. Barnes, and J. Tromp (2000), Wave propagation near a fluid-solid interface: A spectral-element approach, *Geophysics*, *65*(2), 623–631.

Longuet-Higgins, M. S. (1950), A theory of the origin of microseisms, *Philos. Trans. R. Soc. London, Ser. A*, *243*(857), 1–35.

Obrebski, M., F. Ardhuin, E. Stutzmann, and M. Schimmel (2012), How moderate sea states can generate loud seismic noise in the deep ocean, *Geophys. Res. Lett.*, *39*, L11601, doi:10.1029/2012GL051896.

Saito, T. (2010), Love-wave excitation due to the interaction between a propagating ocean wave and the sea-bottom topography, *Geophys. J. Int.*, *182*(3), 1515–1523.

Stacey, R. (1988), Improved transparent boundary formulations for the elastic-wave equation, *Bull. Seismol. Soc. Am.*, *78*(6), 2089–2097.

Stephen, R., P. Bromirski, P. Gerstoft, and P. Worcester (2013), Microseism noise in the Philippine Sea, Abstract S11B-2359 paper presented at 2013 Fall Meeting, AGU, San Francisco, Calif., 9–13 Dec.

Traer, J., P. Gerstoft, P. D. Bromirski, and P. M. Shearer (2012), Microseisms and hum from ocean surface gravity waves, *J. Geophys. Res.*, *117*(B11), B11307, doi:10.1029/2012JB009550.

Tromp, J., D. Komattisch, and Q. Liu (2008), Spectral-element and adjoint methods in seismology, *Commun. Comput. Phys.*, *3*(1), 1–32.

Zhu, J., J. S. Popovics, and F. Schubert (2004), Leaky Rayleigh and Scholte waves at the fluid-solid interface subjected to transient point loading, *J. Acoust. Soc. Am.*, *116*, 2101.